Foliar Lead Uptake by Lettuce Exposed to Atmospheric Fallouts

GAËLLE UZU,[†] SOPHIE SOBANSKA,[‡] GÉRALDINE SARRET,[§] MANUEL MUÑOZ,[||] AND CAMILLE DUMAT*,[†]

Université de Toulouse; INPT, UPS; Laboratoire d'Ecologie Fonctionnelle (EcoLab); ENSAT, av. l'Agrobiopole, BP 32607, 31326 Castanet-Tolosan Cedex, France, LASIR, (UMR CNRS 8516) Université de Lille 1, Bât. C5−59655 Villeneuve d'Ascq cedex, France, Environmental Geochemistry Group, LGIT (UMR 5559), Université J. Fourier and CNRS, 38041 Grenoble cedex 9, France, and Mineralogy and Environments group, LGCA (UMR 5025), OSUG, Université J. Fourier, 1381 rue de la Piscine, 38041 Grenoble cedex 9, France

Metal uptake by plants occurs by soil−root transfer but also by direct transfer of contaminants from the atmosphere to the shoots. This second pathway may be particularly important in kitchen gardens near industrial plants. The mechanisms of foliar uptake of lead by lettuce (*Lactuca sativa*) exposed to the atmospheric fallouts of a lead-recycling plant were studied. After 43 days of exposure, the thoroughly washed leaves contained 335 ± 50 mg Pb kg^{-1} (dry weight). Micro-X-ray fluorescence mappings evidenced Pb-rich spots of a few hundreds of micrometers in diameter located in necrotic zones. These spots were more abundant at the base of the central nervure. Environmental scanning electron microscopy coupled with energy dispersive X-ray microanalysis showed that smaller particles (a few micrometers in diameter) were also present in other regions of the leaves, often located beneath the leaf surface. In addition, submicrometric particles were observed inside stomatal openings. Raman microspectrometry analyses of the leaves identified smelter-originated Pb minerals but also secondary phases likely resulting from the weathering of original particles. On the basis of these observations, several pathways for foliar lead uptake are discussed. A better understanding of these mechanisms may be of interest for risk assessment of population exposure to atmospheric metal contamination.

Introduction

Particles emitted in the atmosphere present a large variety of sizes (*1*), and during the past decade, the proportion of fine particle matter (PM) increased with the use of more effective filters in industry (*2*). PM_{10} (PM for which the aerodynamic diameter is less than 10 μm) are target species of the World Health Organization (*3*) and the European Union Framework Directive on ambient air quality assessment (*4*) due to their adverse effects on the environment and human health. While $PM_{2.5}$, PM_1, and nanoparticles are minor components of total emitted particles, they are probably the most important in terms of environmental impact. Indeed, they can be transported over long distances in the troposphere (*5, 6*), and due to their high specific area, they can strongly impact the biosphere (*7, 8*).

At the global scale, fallouts of atmospheric PM represent the main source of lead pollution in soils (*9*). Despite the strong decrease in industrial and vehicle lead emissions in recent decades (*10*), lead-enriched PM are still emitted in the environment, especially by lead-recycling facilities (*11–13*). In a previous study on particles rejected by such a facility, a large proportion of submicrometric size particles was observed (*7*). Toxic for living organisms even at low concentrations (*14*), lead can be ingested as polluted soil and dust particles by children (*15*). Additional routes of exposure, which are more important for adults, include drinking water contamination and consumption of locally produced vegetables grown in kitchen gardens (*16*).

Lead is known to be weakly mobile in soils (*17, 18*), with a residence time estimated to several hundreds of years (*19*). Lead concentrations in vegetables from kitchen gardens contaminated by atmospheric PM are not correlated with soil contents (*20*). The main reason is that plant uptake is correlated to the phytoavailable fraction of lead rather than to the total metal burden. However, this absence of correlation may be due to a direct metal contamination through the shoots. Airborne contamination of plants by lead and other metals (*21–23*) and by radionuclides (*24*) was evidenced in previous studies. However, the mechanisms responsible for the foliar uptake are still unclear, and the literature on this topic is very limited compared to soil−root transfer. Most studies on foliar transfer concern plant nutrients in the context of foliar fertilization (*25–28*), and to our knowledge there is no study on the mechanisms of foliar uptake of lead.

Terrestrial plants have kept from their aquatic ancestors the ability to absorb nutrients through the leaves (*25*), and contaminants may follow the same pathway. Nutrients and contaminants have to cross several physical barriers before entering the cytosol of epidermal cells. This penetration is strongly dependent on weather conditions, plant species, physiological status, and speciation of the element (*26*). There are two parallel routes for crossing the cuticle, the lipophilic and the hydrophilic pathways (*29, 30*). The lipophilic pathway is not considered in this study because it concerns apolar and noncharged molecules, which cross the cuticle by diffusion in cutin and waxes. Ions and hydrophilic solutes follow the hydrophilic pathway via aqueous pores (*29*). This pathway requires dissolution of the compounds, which depends mostly on the humidity and on the hygroscopicity and solubility of the particles (*26*). When the humidity is above the point of deliquescence, the compound partly dissolves and penetration proceeds from this saturated solution. Aqueous pores are located over anticlinal walls and on cuticular ledges of stomata guard cells (*30, 31*). Once a contaminant has crossed the cuticle, it may remain in the apoplasm or be transported inside cells (*32*). Beside this hydrophilic pathway for solutes, a solid-state pathway also exists. Stomata enable the uptake of suspended nanoparticles and their diffusion in the apoplasm. The stomatal pathway is considered as highly capacitive because of its large size exclusion limit of 10 nm−1 μm and its high transport velocity (*33*).

The first objective of the present study was to evaluate the transfer of lead from atmospheric contamination in lettuce, a widely cultivated vegetable already used as a model plant in metal transfer studies (*16, 34, 35*). Second, this work

* Corresponding author phone: 0033562193903; fax: 0033562193901; e-mail: camille.dumat@ensat.fr.
[†] Université de Toulouse and CNRS.
[‡] Université de Lille 1 and CNRS.
[§] Université J. Fourier and CNRS.
[||] Université J. Fourier.

aimed at investigating the mechanisms of lead foliar uptake by monitoring Pb leaves content over a 43-day exposure time and determining its localization and speciation in the leaves. Such knowledge can be of high interest for risk assessment. Lettuces that were first exposed to the fallouts of a plant recycling batteries emitting lead-rich particles (333 000 mg Pb/kg particles) have been previously characterized (*7*). The total content of lead in the leaves was determined after carefully washing. Micro-X-ray fluorescence (μXRF) was used to study the distribution of lead and other elements on centimetric zones of leaves with a lateral resolution of 50 μm. Environmental scanning electron microscopy coupled with energy dispersive X-ray microanalysis (ESEM−EDX) was used to determine the morphology and elemental composition of lead deposits at a higher resolution, and Raman microspectrometry (RMS) provided the molecular composition of lead-rich areas. The results obtained were then discussed and possible scenarios for lead foliar uptake were proposed. To our knowledge, this is the first study of foliar transfer of metals on vegetable samples originating from a field study using a combination of physical and chemical techniques.

Experimental Section

Lettuce Exposure to Atmospheric Lead Fallouts. Commercial lettuce seeds, "Batavia blonde dorée" cultivar, were surface sterilized with 0.9% CaClO for 15 min and rinsed with deionized water. Lettuces were first grown hydroponically for 10 days before transfer in pots in a greenhouse for 15 days to get plants of about 15 g (fresh biomass). After this period, 40 lettuces were placed in pots containing 4 kg of uncontaminated calcareous soil (total lead concentration 25 $\pm$ 2 mg kg^{-1}). Each pot contained one plant. A geotextile membrane was placed on the soil surface to protect it against atmospheric fallouts. Plants were exposed for 43 days in the courtyard of a secondary lead smelter which recycles batteries (*7*). Every 10 days, five replicates were harvested. In addition, five control plants placed in an urban area 15 km from the smelter were harvested after 43 days. Lead concentration in the courtyard of the recycling plant was 1 μg Pb m^{-3} air and lead concentration in PM emissions was 330 000 mg Pb kg^{-1}. According to the French authorities (*36*), 328 kg of total suspended particles (TSP) including 31 kg of lead were emitted by this facility in 2007. The particles emitted by this smelter were characterized in a previous study by X-ray diffraction and Raman spectroscopy (*7*). Lead speciation was, in decreasing order of abundance, PbS, $PbSO_4$, $PbO \cdot PbSO_4$, α-PbO, and Pb^0.

Chemical Analysis of Soils and Vegetables. After harvesting and removal of the roots, the shoot biomass was measured. Each lettuce was cut in four quarters and one was randomly picked for analyses. The leaves were cut at their base, and each one was washed, first in running tap water for 30 s and then in two baths of deionized water for 1 min, in order to eliminate particles present on the leaf surface but not tightly bound. After draining the leaves with a salad-spinner and drying at 50 °C for 48 h, leaf and soil samples were digested, in a 1:1 mixture of HNO_3 and H_2O_2 at 80 °C for 4 h and in hot aqua regia, respectively. After filtration, lead concentration was measured by inductively coupled plasma atomic emission spectrometry (ICP-AES) with an IRIS Intrepid II XDL. The accuracy of the acidic digestion and analytical procedures was checked using the reference material Virginia tobacco leaves, CTA-VTL-2, ICHTJ. The certified value for lead in tobacco leaves was given as 22.1 $\pm$ 1.2 mg Pb kg^{-1} dry weight. Measured values for the three replicates were 22.0 $\pm$ 0.9, 22.4 $\pm$ 0.8, and 21.9 $\pm$ 0.8 mg Pb kg^{-1} dry weight. The leaves of the lettuces after 43 days of exposure were then studied by μXRF, ESEM−EDX, and RMS.

Micro-X-ray Fluorescence (μXRF). Elemental distributions in various regions of the leaves were determined by μXRF. Fresh washed leaves were freeze-dried, flattened on the sample holder, and placed under vacuum. μXRF spectra were collected with an EDAX Eagle III XRF spectrometer, equipped with a Rh anode and a polycapillary that focuses the X-ray beam down to 30 μm full width at half-maximum (FWHM). An EDX detector with 140 eV resolution was used to measure the X-ray fluorescence. The spectrometer was operated at 15 or 20 kV and 300−450 μA. Centimetric sized X-ray maps were collected over 256 by 200 pixels with steps of 30−50 μm. The counting time was 600−2000 ms per pixel. Detection limits for such apparatus is around 100 ppm for Pb and other heavy elements. Deconvolution of μXRF spectra was needed since the S K- and Pb M-lines overlap within the 140 eV resolution of the EDX detector (Figure 1b). It was performed using the EDAX-integrated software Vision32. Despite the peak overlap, the statistics on Pb fluorescence signal were better using the Pb M-line than the Pb L-line at higher voltage (40 kV). Elemental maps were combined as RGB (red−green−blue) three-color maps using Matlab. In addition, the XRF spectra for the Pb-rich particles obtained by summing single-pixel spectra in the spot of interest were compared.

Environmental Scanning Electron Microscope (ESEM−EDX). Morphology and elemental distribution were studied using an ESEM (Quanta 200 FEI) equipped with a Quantax EDX detector (Rontec). It was operated at 25 kV in the low vacuum mode. Semiquantification measurements were obtained with ZAF correction and using real standards. Leaves were air-dried and fixed on a carbon substrate before analysis. As for the μXRF analyses, Pb M-peaks and S K-peaks were separated by deconvolution.

Raman Microspectrometry (RMS). Molecular identification of particles present on or beneath the leaf surface of lettuce leaves was performed using RMS. Leaf samples collected after 43 days of exposure were fixed on a glass plate and mounted on the microscope stage without further preparation. In most cases, particles (or leave areas) were analyzed by both ESEM−EDX and RMS after a careful relocalization; thus, electronic and optical images as well as elemental and molecular compositions could be compared. RMS measurements were carried out using a Labram confocal spectrometer and a Labram HR UV 800 (Jobin Yvon, Horiba Gr, France). The Raman backscattering was excited with 632.8 or 266 nm excitation wavelength supplied by a He−Ne and a solid MBD 266 system (Coherent Laser Group), respectively. The beams were focused on the sample surface through an optical objective (visible Olympus objective, ×100, 0.9 NA, and UV Mitutoyo objective ×80, 0.55 NA) with a lateral resolution (*XY*) of less than 1 μm in both cases. The excitation using a UV laser (266 nm) was necessary to probe the surface of leaves, since many biologically important molecules such as chlorophyll have an intense fluorescence emission when excited in the visible range (400 nm < λ < 800 nm). Fluorescence cross sections are typically several orders of magnitude larger than Raman scattering cross-section and masks any underlying Raman spectra. The Raman spectra were analyzed on the basis of the shifts in Raman peak values, changes in full width at half-maximum (FWHM) ratios of Raman bands, and normalized intensity variations. For identification of chemical species, measured Raman spectra (band wavenumber and relative intensities) with flat baseline were compared with spectra in established libraries using Spectral Library Search ID 301 software (Thermo Galactic). The hit quality index (HQI) represents the closeness of the match between the unknown and a particular library entry. Raman spectra libraries used are listed in the Supporting Information. In addition to these databases, Raman spectra of relevant Pb compounds were recorded to check for possible

differences due to instrumental functions. Further information about identification of Pb minerals using RMS can be found elsewhere (*12, 37*).

Statistical Data Treatment. The obtained amount of lead in plants was subjected to analysis of variance (ANOVA) with one factor, using the software Statistica, Edition '98 (StatSoft Inc., Tulsa, OK). Significant differences ($p < 0.05$) were measured by the LSD Fisher test.

Results and Discussion

Foliar Lead Uptake. Pb average concentrations in washed leaves after 0, 13, 23, 34, and 43 days of atmospheric fallouts exposure were 0.22 ± 0.09, 69 ± 15, 139 ± 40, 217 ± 40, and 335 ± 50 mg kg^{-1} dry weight (DW), respectively. These values were all significantly different, and lead enrichment as a function of time followed a linear law, without plateau at 43 days of exposure: $[Pb]_{leaves} = 6.98 \times$ (number of days of exposure), $r^2 = 0.96$, $n = 5$.

No significant difference in leaf biomass was noticed between control and exposed plants (40 ± 5 g DW after 43 days), and plants stayed green and healthy despite some necrotic spots (see below). The comparison of the total lead concentrations in leaves between the exposed and control plants after 43 days (335 ± 50 and 5 ± 3 mg kg^{-1}, DW, respectively) suggests a strong foliar lead uptake by exposed plants. Other lettuces cultivated at 250 and 400 m from the smelter (not investigated in this study) contained 30 and 15 mg kg^{-1}, DW, respectively. Thus, lead content strongly varies as a function of the distance to the smelter. A survey of reported metal contents in vegetables in potentially contaminated sites (*38*) showed a great variability as a function of sampling sites and environmental conditions. According to EU requirements for consumption (*4*), lead concentration should not exceed 0.3 mg Pb kg^{-1} fresh biomass in leaf-vegetables, corresponding to 3.26 mg Pb kg^{-1} DW in our study (DW reached 10.85% in exposed lettuces). Thus, this threshold value was reached after 0.5 day of exposure in the plant courtyard. The relatively high lead content measured in control plants could result from soil−root uptake. However, this latter hypothesis is not likely, because the control soil was chosen for its relatively high pH (8.4) and carbonates amount (98 g kg^{-1}) to minimize Pb availability (*17, 39*) and low lead content. Lead present in the control plant more likely results from diffuse Pb contamination of the urban environment.

After exposure, no variation of lead content in the soil contained in the pots was observed (<30 mg Pb kg^{-1}). However, this is not a proof that Pb root uptake did not occur. Supposing that Pb contained in the control plants only originates from the substrate (which likely overestimates the soil−root transfer), the amount of lead taken up by roots would represent only 1.5% of total Pb measured in the leaves after 43 days of exposure in the plant courtyard. So the soil−root uptake of Pb can be neglected relative to the foliar uptake. In conclusion, the strong Pb enrichment in exposed plants is due to a foliar contamination. Considering that vegetables were thoroughly washed, lead was at least strongly bound to the leaf surface or internalized.

Lead Distribution in the Leaves, Spatially Resolved Speciation, and Phytotoxicity Symptoms. The distribution of lead and other elements was investigated at the leaf-scale by μXRF on 10 leaves on centimetric zones. Figure 1 shows the analysis of the basal part of a leaf. Four lead-rich zones of a few hundreds of micrometers corresponding to brownish necrotic zones were observed (spots 1−4 in Figure 1c). The μXRF spectra for the four spots, obtained by summing single pixel spectra, are shown in Figure 1b. The spots contain the same elements but in varying proportions: Spot 1 is richer in S, Ca, Si, and Fe, whereas spots 2, 3, and 4 are richer in Mn, and spot 4 contains less K. The same type of elemental distributions and grain compositions were observed in other parts of the leaves (Figure S1, Supporting Information). A μXRF map of a Pb-rich necrosis obtained at a higher resolution (20 μm step size) showed that although Ca and Mn present high local concentrations, their distribution does not quite match Pb distribution (Figure S2, Supporting Information). No diffuse lead concentration was detected in the leaf tissue. The detection limit of the instrument is relatively high (around 100 ppm for Pb), so one cannot conclude on the absence of lead in the leaf tissue. Another type of necrosis was observed on the leaves of both control and exposed plants, small black spots rich in Mn (Figure 1d). They are symptoms of Mn toxicity resulting from reductive dissolution due to water saturation phenomenon of the substrate (*40*) and are not related to Pb contamination.

The leaves were then studied at a higher resolution by ESEM−EDX and RMS. A variety of Pb-rich necroses were investiagted (Figures 2a−c and S3, Supporting Information). As shown by μXRF, EDX maps showed a heterogeneous distribution of Pb within a Ca- and Mn-containing phase (Figure 2b). P and K elements were detected in all the necroses, suggesting the presence of an organic membrane covering the precipitates. This organic layer was clearly visible on the secondary electron images (e.g., Figures 2b,c and S3, Supporting Information) and on an optical image (e.g., Figure S4, Supporting Information). The RMS measurements carried out using a laser beam with a wavelength in the visible region showed an intense fluorescence signal typical of organic substances (e.g., chlorophyll). Measurements using a laser beam at 266 nm allowed probing the compounds beneath this organic membrane. The Ca, Mn phase was identified by Raman as a mixed carbonate, i.e., $(Ca_{1-x}Mn_x)CO_3$, thanks to a characteristically intense Raman band at 1087 cm^{-1} corresponding to the symmetric stretching (ν_1) of the carbonate group (symmetry D_{3h}) in the calcite-like structure (space group $R\bar{3}c$). Small particles of MnO_2 and $PbSO_4$ were found within this carbonate precipitate (Figure 2 and Supporting Information). The Raman bands at ~1580 and ~1300 cm^{-1} found on many spectra were assignated to carbonaceous material resulting from the degradation of the organic membrane by the UV laser beam.

Necroses associated with metal accumulations have already been observed for Cd in *Brassica juncea* L. (*41*) and *Thlaspi caerulescens* (*42*) in the case of metal root uptake and for Pb in *Arabidopsis thaliana* in the case of foliar uptake (*43*). Necroses are formed by dead cells and are symptoms of relatively acute toxicity. In the present study, metal-rich necroses suggest a toxic effect of metals (Pb, Zn, Fe, Cu, Mn depending on the spot, Pb being generally the most concentrated one). A likely scenario is the transfer of some metals in the intracellular compartment, leading to interferences with the cell metabolism. Further microscopic investigations are required to confirm this hypothesis.

In all leaves studied, the base of the central vein contained more particles than the other regions of the leaf. This phenomenon is likely due to rainfall and watering, which flushed the particles toward the basal part of the leaves. This was already reported in the case of radionuclide-containing particles (*44*). In order to reduce the risk induced by vegetables potentially exposed to atmospheric fallouts, a simple recommendation could consist of eliminating the basal part of leaves before consumption.

Particles were also present on the leaf surface (Figure S6, Supporting Information). Individual particles and aggregates observed ranged from a few micrometers to a few tens of micrometers in diameter. The major elements detected by EDX in particles/aggregates were Pb, S, Cl, Fe, Ca, Si, and Al. The RMS analysis of the particles allowed the identification of anglesite ($PbSO_4$), lanarkite ($xPbO \cdot PbSO_4$), quartz (α-SiO_2), amorphous iron oxyhydroxide (FeOOH), calcite ($CaCO_3$),

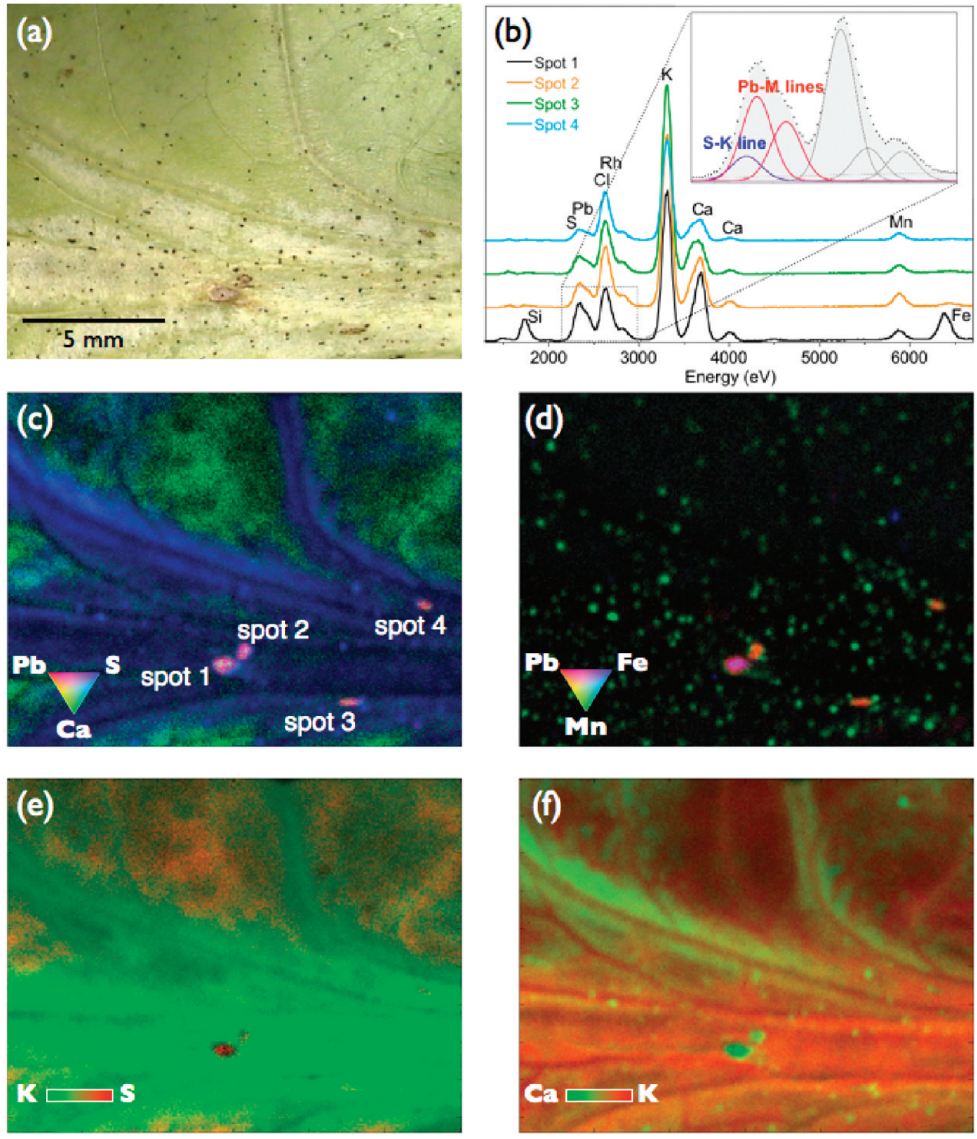

FIGURE 1. (a) Optical image of the basal part of the lettuce leaf exposed to atmospheric fallouts. Brownish spots correspond to Pb-associated necroses. (b) XRF spectra of Pb-rich necroses (spot 1, 2, 3, 4). Tricolor and bicolor μXRF elemental maps for Ca, Pb, and S (c), Fe, Pb, and Mn (d), K and S (e), and Ca and K (f).

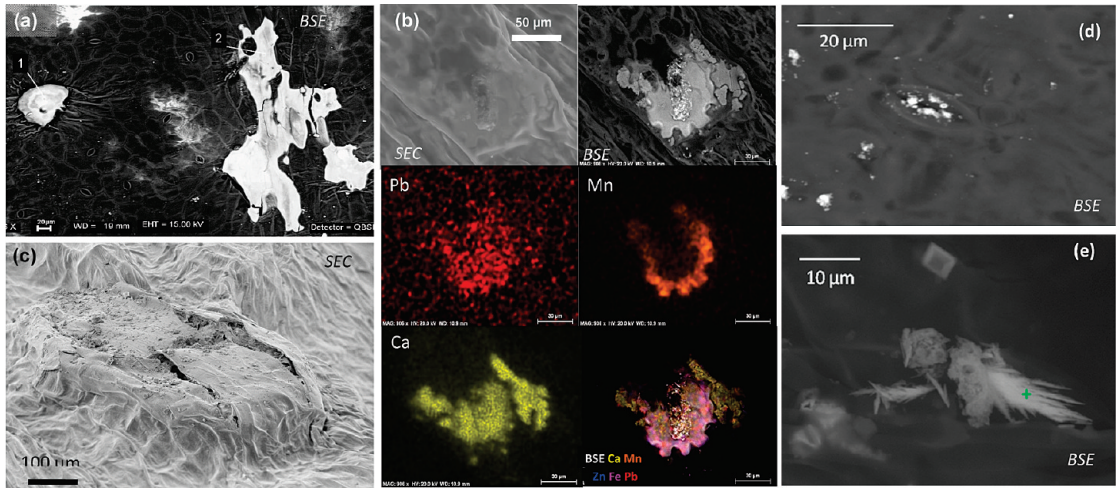

FIGURE 2. ESEM–EDX analyses of Pb-rich regions on lettuce leaves exposed to atmospheric fallouts. (a) Two large necroses are shown in BSE mode. The EDX semiquantification for spots 1 and 2 gave 9% Pb, 1% Cl, 1% Mn, 1% Fe, 20% O, 2% Mg, and 65% P. (b) SE and BSE images of a necrosis; elemental distribution of Pb, Ca, and Mn; and multicolor map showing the distribution of Ca, Mn, Zn, Fe and Mn. (c) SE image of a necrosis. Particles are visible on the leaf surface, as well as beneath the surface. (d) Stomata plugged by Pb-containing particles. (e) Secondary Pb-containing compounds formed on the leaf surface.

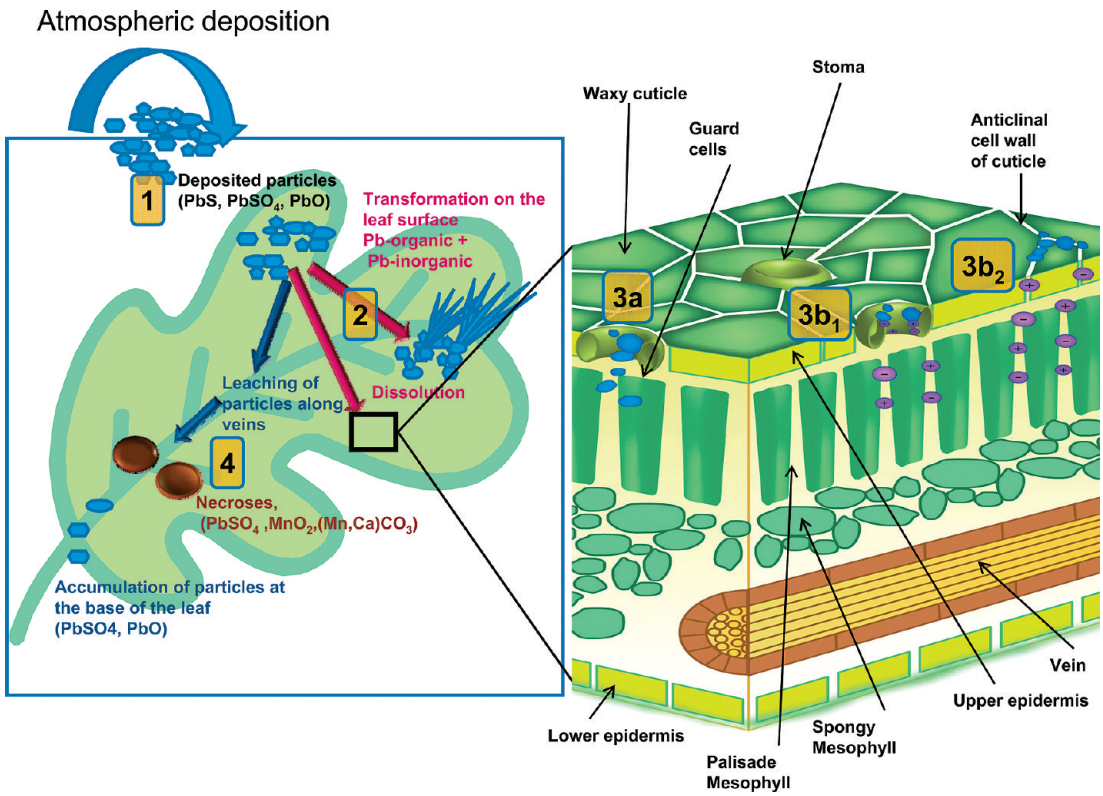

FIGURE 3. Tentative pathways for lead uptake after deposition of Pb-containing particles. Deposition of particles on the leaf surface (1), chemical transformation on the leaf surface leading to secondary Pb-containing phases and possibly solutes (2). Accumulation of particles in stomata and possibly penetration of nanoparticles (3a). Possible diffusion of solutes via aqueous pores present on cuticular ledges of stomata ($3b_1$) and anticlinal cell walls of cuticles ($3b_2$). Toxicity symptoms (necroses) induced by the presence of the contaminated particles on the leaf (4).

hydrocerussite ($Pb_3(CO_3)_2(OH)_2$), cerussite ($PbCO_3$), and some fluorescent species attributed to clay minerals (Figure S7, Supporting Information). Clay may result from the deposition of noncontaminated soil dust particles. PbS was not detected because this mineral is almost silent in Raman (a weak and broad Raman band is observed at 451 cm^{-1}), and this compound readily transforms into lead sulfate products under the laser beam (*45*).

PM were also frequently observed inside stomatal openings on adaxial and abaxial surfaces (Figures 2d and S8, Supporting Information). These PM had a diameter between 50 nm and 1 μm, and minerals identified by RMS included $PbSO_4$ and PbO. The presence of these particles in stomata may have two consequences. First, clogging ostioles disturbs leaf physiology by decreasing the stomatal conductance and gas exchanges and perturbing the water regime, transpiration, and control of leaf temperature (*46*). Second, toxic metals may penetrate inside leaves via stomata (*33*).

Although some aggregates presented the same morphology as source particles characterized previously (*7*), 3−4% of needle crystallites were observed on leaf surface (ratio of needlelike particles to the total number of particles observed, Figures 2e and S9, Supporting Information). These crystallites were not observed in source particles (*7*). EDX analyses showed Pb, K, and Cl as major constituents of the needle structures, whereas other elements such as Sn, Ca, K, and Fe were found in nonspherical particles associated with the needles. These crystallites were not made of lead phosphate. RMS measurements showed that they were very beam sensitive and intense PbO and elemental carbon signals were observed after beam damage. These observations suggest that the needles are made of lead−organic species. This was confirmed by spectra recorded at very low laser power on which not very intense Raman bands at ~2800 and ~ 1780 cm^{-1} characteristic of C−H and C−O bonds, respectively, were observed. These particles may correspond to secondary phases resulting from the dissolution of original particles on the leaf and precipitation with organic compounds present on the cuticle. These changes in particles' morphology and speciation may result from abiotic processes. However, the surface of plant leaves is generally colonized by microorganisms that may participate in chemical processes taking place at this interface (*47, 48*). Further investigations are required to evaluate the bacterial colonization on the lettuce leaves and the possible participation of microorganisms in the alteration of the particles.

Potential Mechanisms Involved in Foliar Uptake. The results of this study clearly show that some lead is trapped both on the leaf surface and inside the leaf. On the basis of our observations and on the present knowledge on foliar uptake of elements, several mechanisms can be tentatively proposed for these processes (Figure 3). First, particles deposited on the leaf surface may be trapped in the tiny folds of the leaf and remain as such. The original particles contain PbS, which is highly reactive and subject to oxidation and weathering processes, and secondary Pb-containing compounds may form on the leaf surface. The chemical processes of PbS oxidation under atmospheric conditions have been described previously (*45, 49*) and lead to the formation of PbO, $PbSO_4$, $PbO{\cdot}PbSO_4$, and $PbCO_3$. These transformations may occur in the atmosphere during the transport of particles and after their deposition on plant leaves. In parallel, lead may penetrate inside the leaf by two pathways. First, lead-containing nanoparticles observed in the stomata may penetrate in the apoplasm as solid compounds. In this study, nanoparticles were observed only in stomatal openings. Further analyses, particularly the study of leaf cross sections, are necessary to test whether nanoparticles enter the leaves via stomata. In addition, particles were observed beneath an organic membrane, probably the

cuticle. Again, further investigations are needed to determine their exact localization and the way they were transferred in this place. Second, lead resulting from the dissolution of source particles may diffuse through aqueous pores of the cuticle and of the stomata, following the hydrophilic pathway, inducing the formation of necroses enriched with lead.

Our results suggest that various pathways may lead to foliar uptake of Pb by lettuce exposed to Pb-rich PM. The fate of metal contaminants in the soil and their soil−plant transfer has to be evaluated in metal-contaminated soils, but the foliar transfer is another important issue, which is much less studied. Indeed, in the context of agricultural activities established near metallurgic activities, plant metal uptake may occur predominantly via foliar contamination by micro- and nanoparticles. Microscopic and microspectroscopic investigations of the plants provided insights on the fate of PM deposited on lettuce leaves. Such knowledge may be of interest from a physiological point of view and from the perspective of risk assessment of atmospheric emissions in urban environments.

Acknowledgments

ADEME (the French Agency for Environment and Energy) and the STCM are acknowledged for their financial support and technical help. This research project was supported by the National CNRS CYTRIX-EC2CO program. We thank M. Boidot for Figure 3, P. Recourt from Laboratoire Geosystèmes, UMR CNRS 8157, Université de Lille 1 au lieu de, for ESEM−EDX measurements, and M. Corazzi for his help during the μXRF measurements.

Supporting Information Available

Additional information as noted in the text. This material is available free of charge via the Internet at http://pubs.acs.org.

Literature Cited

(1) Zhang, Z.; Kleinstreuer, C.; Donohue, J.; Kim, C. Comparison of micro- and nano-size particle depositions in a human upper airway model. *J. Aerosol Sci.* **2005**, *36*, 211–233.

(2) Müller, D.; Mattis, I.; Kolgotin, A.; Ansmann, A.; Wandinger, U.; Althausen, D. Characterization of atmospheric aerosols with multiwavelength Raman lidar. In *Proceedings of SPIE, Florence, Italy*; 2007; 67500G-67500G-11.

(3) WHO. Air Quality Guidelines for Europe European Series. 1987, number 23.

(4) European Commission. Commission Regulation (EC) No 221/2002 of 6 February 2002 amending regulation (EC) no. 466/2001 setting maximum levels for certain contaminants in foodstuffs. 2002.

(5) Dordevic, D.; Vukmirovic, Z.; Tosic, I.; Unkasevic, M. Contribution of dust transport and resuspension to particulate matter levels in the Mediterranean atmosphere. *Atmos. Environ.* **2004**, *38*, 3637–3645.

(6) Arimoto, R. Eolian dust and climate: Relationships to sources, tropospheric chemistry, transport and deposition. *Earth-Sci. Rev.* **2001**, *54*, 29–42.

(7) Uzu, G.; Sobanska, S.; Aliouane, Y.; Pradere, P.; Dumat, C. Study of lead phytoavailability for atmospheric industrial micronic and sub-micronic particles in relation with lead speciation. *Environ. Pollut.* **2009**, *157*, 1178–1185.

(8) Fernandez Espinosa, A. J.; Oliva, S. R. The composition and relationships between trace element levels in inhalable atmospheric particles (PM10) and in leaves of *Nerium oleander* L. and *Lantana camara* L. *Chemosphere* **2006**, *62*, 1665–1672.

(9) Donisa, C.; Mocanu, R.; Steinnes, E.; Vasu, A. Heavy metal pollution by atmospheric transport in natural soils from the northern part of Eastern Carpathians. *Water, Air Soil Pollution.* **2000**, *120*, 347–358.

(10) Glorennec, P.; Bemrah, N.; Tard, A.; Robin, A.; Bot, B. L.; Bard, D. Probabilistic modeling of young children's overall lead exposure in France: Integrated approach for various exposure media. *Environ. Int.* **2007**, *33*, 937–945.

(11) Sobanska, S.; Ledesert, B.; Deneele, D.; Laboudigue, A. Alteration in soils of slag particles resulting from lead smelting. *Compt. Rend. Acad. Sci.—Series IIA* **2000**, *331*, 271–278.

(12) Batonneau, Y.; Bremard, C.; Gengembre, L.; Laureyns, J.; Le Maguer, A.; Le Maguer, D.; Perdrix, E.; Sobanska, S. Speciation of PM10 sources of airborne nonferrous metals within the 3-km zone of lead/zinc smelters. *Environ. Sci. Technol.* **2004**, *38*, 5281–5289.

(13) Ohmsen, G. S. Characterization of fugitive material within a primary lead smelter. *J. Air Waste Manage. Assoc.* **2001**, *51*, 1443–1451.

(14) Canfield, R. L.; Henderson, C. R.; Cory-Slechta, D. A.; Cox, C.; Jusko, T. A.; Lanphear, B. P. Intellectual impairment in children with blood lead concentrations below 10 μg per deciliter. *N. Engl. J. Med.* **2003**, *348*, 1517–1526.

(15) Alloway, B. J. *Heavy Metals in Soils*, 2nd ed.; Blackie Academic & Professional: London, 1995.

(16) Alexander, P.; Alloway, B.; Dourado, A. Genotypic variations in the accumulation of Cd, Cu, Pb and Zn exhibited by six commonly grown vegetables. *Environ. Pollut.* **2006**, *144*, 736–745.

(17) Cecchi, M.; Dumat, C.; Alric, A.; Felix-Faure, B.; Pradere, P.; Guiresse, M. Multi-metal contamination of a calcic cambisol by fallout from a lead-recycling plant. *Geoderma* **2008**, *144*, 287–298.

(18) Dumat, C.; Chiquet, A.; Gooddy, D.; Aubry, E.; Morin, G.; Juillot, F.; Benedetti, M. F. Metal ion geochemistry in smelter impacted soils and soil solutions. *Bull. Soc. Geol. Fr.* **2001**, *172*, 539–548.

(19) Klaminder, J.; Bindler, R.; Laudon, H.; Bishop, K.; Emteryd, O.; Renberg, I. Flux rates of atmospheric lead pollution within soils of a small catchment in northern Sweden and their implications for future stream water quality. *Environ. Sci. Technol.* **2006**, *40*, 4639–4645.

(20) Douay, F.; Roussel, H.; Pruvot, C.; Loriette, A.; Fourrier, H. Assessment of a remediation technique using the replacement of contaminated soils in kitchen gardens nearby a former lead smelter in Northern France. *Sci. Total Environ.* **2008**, *401*, 29–38.

(21) Tjell, J. C.; Hovmand, M. F.; Mosbaek, H. Atmospheric lead pollution of grass grown in a background area in Denmark. *Nature* **1979**, *280*, 425–426.

(22) Mosbaek, H.; Tjell, J. C.; Hovmand, M. F. Atmospheric lead input to agricultural crops in Denmark. *Chemosphere* **1989**, *19*, 1787–1799.

(23) Kozlov, M. V.; Haukioja, E.; Bakhtiarov, A. V.; Stroganov, D. N.; Zimina, S. N. Root versus canopy uptake of heavy metals by birch in an industrially polluted area: contrasting behavior of nickel and copper. *Environ. Pollut.* **2000**, *107*, 413–420.

(24) Madoz-Escande, C.; Henner, P.; Bonhomme, T. Foliar contamination of *Phaseolus vulgaris* with aerosols of 137Cs, 85Sr, 133Ba and 123mTe: Influence of plant development stage upon contamination and rain. *J. Environ. Radioact.* **2004**, *73*, 49–71.

(25) Mengel, K. Alternative or complementary role of foliar supply in mineral nutrition In *Proceedings of the International Symposium on Foliar Nutrition of Perennial Fruit Plants*; Tagliavini, M., Toselli, M., Bertschinger, L., Neilsen, D. Thalheimer, M., Eds.; International Society Horticultural Science: Leuven, Belgium, 2002; pp 33−47.

(26) Schönherr, J.; Luber, M. Cuticular penetration of potassium salts: Effects of humidity, anions, and temperature. *Plant Soil* **2001**, *236*, 117–122.

(27) Ferrandon, M.; Chamel, A. Foliar uptake and translocation of iron, zinc and manganese—Influence of chelating-agents. *Plant Physiol. Biochem.* **1989**, *27*, 713–722.

(28) Chamel, A.; Bougie, B. Foliar uptake of copper—Studies on cuticular sorption and penetration. *Vegetal Physiol.* **1977**, *15*, 679–693.

(29) Schönherr, J. Calcium chloride penetrates plant cuticles via aqueous pores. *Planta* **2000**, *212*, 112–118.

(30) Schonherr, J. Characterization of aqueous pores in plant cuticles and permeation of ionic solutes. *J. Exp. Bot.* **2006**, *57*, 2471–2491.

(31) Eichert, T.; Burkhardt, J. Quantification of stomatal uptake of ionic solutes using a new model system. *J. Exp. Bot.* **2001**, *52*, 771–781.

(32) Chamel, A.; Pineri, M.; Escoubes, M. Quantitative determination of water sorption by plant cuticles. *Plant, Cell Environ.* **1991**, *14*, 87–95.

(33) Eichert, T.; Kurtz, A.; Steiner, U.; Goldbach, H. E. Size exclusion limits and lateral heterogeneity of the stomatal foliar uptake pathway for aqueous solutes and water-suspended nanoparticles. *Physiol. Plant.* **2008**, *134*, 151–160.

(34) Waisberg, M.; Black, W. D.; Waisberg, C. M.; Hale, B. The effect of pH, time and dietary source of cadmium on the bioaccessibility and adsorption of cadmium to/from lettuce (*Lactuca sativa* L. cv. Ostinata). *Food Chem. Toxicol.* **2004**, *42*, 835–842.

(35) Khan, S.; Aijun, L.; Zhang, S.; Hu, Q.; Zhu, Y. Accumulation of polycyclic aromatic hydrocarbons and heavy metals in lettuce grown in the soils contaminated with long-term wastewater irrigation. *J. Hazard. Mater.* **2008**, *152*, 506–515.
(36) DRIRE. Direction régionale de l'industrie de la recherche et de l'environnement. http://www.drire.gouv.fr/midi-pyrenees/.
(37) Sobanska, S.; Ricq, N.; Laboudigue, A.; Guillermo, R.; Bremard, C.; Laureyns, J.; Merlin, J. C.; Wignacourt, J. P. Microchemical investigations of dust emitted by a lead smelter. *Environ. Sci. Technol.* **1999**, *33*, 1334–1339.
(38) BAPPET-Database on ETM in vegetables. ADEME, INERIS, CNAM, INP, ENSAT, ISA, 2008 (http://www.sites-pollues.developpement-durable.gouv.fr/DocumentsDiagnostics.asp#BAPPET).
(39) Birkefeld, A.; Schulin, R.; Nowack, B. In situ transformations of fine lead oxide particles in different soils. *Environ. Pollut.* **2007**, *145*, 554–561.
(40) Foy, C. D.; Chaney, R. L.; White, M. C. The physiology of metal toxicity in plants. *Annu. Rev. Plant. Physiol.* **1978**, *29*, 511–566.
(41) Salt, D. E.; Prince, R. C.; Pickering, I. J.; Raskin, I. Mechanisms of cadmium mobility and accumulation in Indian mustard. *Plant Physiol.* **1995**, *109*, 1427–1433.
(42) Cosio, C.; DeSantis, L.; Frey, B.; Diallo, S.; Keller, C. Distribution of cadmium in leaves of *Thlaspi caerulescens*. *J. Exp. Bot.* **2005**, *56*, 765–775.
(43) Lummerzheim, M. S. Comparative microscopic and enzymatic characterization of the leaf necrosis induced in *Arabidopsis thaliana* by lead nitrate and by *Xanthomonas campestris* pv. campestris after foliar spray. *Plant, Cell Environ.* **1995**, *18*, 499–509.
(44) Madoz-Escande, C.; Santucci, P. Weather-dependent change of cesium, strontium, barium and tellurium contamination deposited as aerosols on various cultures. *J. Environ. Radioact.* **2005**, *84*, 417–439.
(45) Batonneau, Y.; Bremard, C.; Laureyns, J.; Merlin, J. C. Microscopic and imaging Raman scattering study of PbS and its photo-oxidation products. *J. Raman Spectrosc.* **2000**, *31*, 1113–1119.
(46) Hirano, T.; Kiyota, M.; Aiga, I. Physical effects of dust on leaf physiology of cucumber and kidney bean plants. *Environ. Pollut.* **1995**, *89*, 255–261.
(47) Andrews, J. H.; Harris, R. F. The ecology and biogeography of microorganisms on plant surfaces. *Annu. Rev. Phytopathol.* **2000**, *38*, 145–180.
(48) Lindow, S. E.; Brandl, M. T. Microbiology of the phyllosphere. *Appl. Environ. Microbiol.* **2003**, *69*, 1875–1883.
(49) Choel, M.; Deboudt, K.; Flament, P.; Lecornet, G.; Perdrix, E.; Sobanska, S. Fast evolution of tropospheric Pb- and Zn-rich particles in the vicinity of a lead smelter. *Atmos. Environ.* **2006**, *40*, 4439–4449.